EPJ Web of Conferences **266**, 13015 (2022)
EOSAM 2022
https://doi.org/10.1051/epjconf/202226613015

Comparison of simulation and experimental characterization of a 4-pass diode-pumped 4-active-mirrors 1053 nm laser amplifier

Thomas Hamoudi[1], Hugo Chesneau[1], Thomas Dubé[1], Emma Dubois[1], Manon Lamy[1], Cédric Maunier[1], Alain Braud[2], Cesare Meroni[2], Patrice Camy[2], Sébastien Montant[1] *

[1] *CEA,CESTA, F-33116 Le Barp, France*

[2] *CIMAP-ENSICAEN, 6 Boulevard du Maréchal Juin, 14050 Caen Cedex, France*

Abstract. In this paper, we will discuss the performances of a 4-pass diode-pumped 4-active-mirrors laser amplifier. Numerical simulations along with experimental characterization paves the way to reach 1 J at 10 Hz pulse rate at 1053 nm. Both Nd :glass and Nd :Lu :CaF_2 amplifier medium performances will be compared in this amplifier.

1 Context

The Laser MegaJoule (LMJ) is a French laser facility designed to perform extreme laser-matter interaction Physics. Each of the 22 laser chains is injected by a front-end composed of a master oscillator fiber amplifier and a bulk Pre Amplifier Module (PAM). The nJ pulse yielded by the fiber seeder is consecutively amplified by the regenerative and the 4-pass amplifiers of the PAM up to 1 J. In this paper, we will draw comparisons between simulations and experiments of the 4-pass diode-pumped 4 active-mirrors laser amplifier to overcome thermal effects in order to achieve 1 J at 10 Hz.

2 Amplifier architecture

2.1 Geometry of laser medium

To reach energies at the joule level, two types of laser materials geometry can be used: rod and thin disk. Some architectures of rod amplifiers have shown the possibility of obtaining energies close to the joule [1, 2]. However, surface/volume ratio of this rod geometry lead to important harmful thermal effects. For example, in the Laser MegaJoule preamplifier, thermal effects occurring in the flashlamp-pumped Nd-doped phosphate glass rod of the 4-pass amplifier limits the 1 Hz repetition rate of the regenerative amplifier to 1 shot every 5 min. Generally, thermal effects may appear as wavefront deformation [3]. To counteract thermal effects in the amplifier rods in high power laser, thin-disk amplifiers have been developed. With an interesting surface/volume ratio, extraction of heat capacity is optimal, hence thermal effects are limited. However, sub-millimeter thin-disk thickness triggers a lower gain per pass. A trade-off was made with the development of active-mirrors amplifiers (AMA), having a millimeter thickness. Thus, AMA have been demonstrated to be sustainable amplifiers for use in high energy laser [4, 5, 6].

2.2 Gain medium

In addition to the architecture modification to increase the heat extraction, a new gain medium is used. For equivalent laser parameters, CaF_2 codoped with Nd^{3+} et Lu^{3+} exhibits a 4.3 W/m/K thermal conductivity which is seven time higher compared to Nd-doped phosphate glass [7]. Longitudinal pumping of the AMA enforces high homogeneity of the pump beam profile to obtain a good homogeneity of the spatial gain. We design an optimized hollow duct (HD) consisting of a funnel-shaped part to shape the pump beam and a waveguide to optimize its homogeneity. Several configurations with collimated or non-collimated pump diodes have been compared along with experiments and simulations in terms of efficiency, homogeneity and gain.

3 One active-mirror characterization

3.1 Wavefront distortion

Firstly, we have to characterize the wavefront distortion of the new lasers materials. For this, one AMA is pumped by a laser diode with a top-hat square profile. A probe beam at 1053 nm is seeded into the AMA during pumping. Then, the probe laser is analyzed with a Shack-Hartmann wavefront sensor (SHWS). 5 active mirrors have been characterized: Nd: Phosphate with a thickness of 3 and 5 mm and 0.5%Nd:x%Lu:CaF_2 active-mirrors with x equals to 5%, 6.5% and 8% with a thickness of 4 mm.

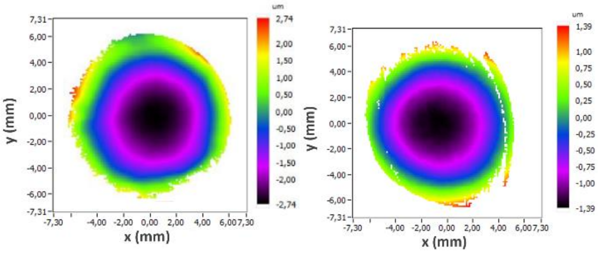

Figure 1 : Wavefront distortion measurment of 0.5%Nd: 5%Lu : CaF_2 at 10 Hz repetition rate (left) and Nd :Phosphate at 4 Hz repetition rate (right) active-mirror.

Figure 1 shows the wavefront distortion measured by SHWS of Nd: 5%Lu: CaF_2 and Nd: Phosphate active-mirror of 4 and 5 mm thickness respectively, with 1.6 J of pump energy at 4 Hz and 10 Hz respectively. The wavefront displays almost spherical thermal lens in

* Corresponding author: sebastien.montant@cea.fr

contrast with transversely pumped rod amplifier [3]. However, the peak-to-valley curvature value is higher for Nd: Phosphate than Nd: Lu: CaF_2 (5.48 µm vs 2.78 µm).

3.2 Hollow-Duct development

To optimize efficiency and homogeneity of the pump beam, a spatial diode shaping system has been developed. This hollow duct is composed of two distinct parts: a funnel to shape and a waveguide to homogenize the pump beam. To limit reflection losses, a gold coating is applied on the hollow duct. At the output of this HD, the pump beam is top-hat with a 8x8mm² square shape. Finally, different sizes of the funnel and waveguide have been compared. An influence has been shown on the gain and its spatial homogeneity with the different sizes. The gain homogeneity have been measured with a spatially resolved gain measurement. A trade-off was made between these two parameters to obtain a gain of 1.4 per pass with 4 J of pump energy with a good spatial homogeneity.

3.3 4-pass 1-active-mirror demonstration

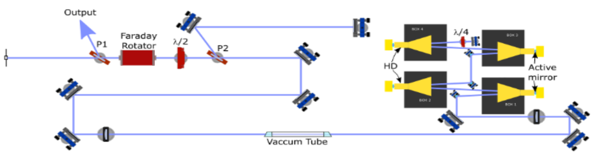

Figure 2. 4-pass amplifier scheme with P: polarizer, HD : hollow duct, λ/2 : half wave plate.

Figure 2 outlines the general scheme of the 4-pass amplifier, with 4 AMA each longitudinally pumped with 2 collimated diode stacks.

This 4-pass amplifier is seeded with 10 mJ, 1053 nm central wavelength, circular gaussian profile regenerative amplifier. A serrated aperture picks an almost square top-hat profile. The square pump beam and laser dimension are 8x8mm² and 6x6mm² respectively. All active-mirrors have a diameter of 15 mm and a thickness of 5 mm. They are each glued to copper heatsinks water-cooled at 20°C. One AMA is placed on a 4 axes precision positioning gimbal mount, with 2 rotation and 2 translation stages. The formers are used to optimize the position of the AMA center on the laser beam during pumping. Indeed, the absorption of pump beam induced an almost curvature wavefront distortion on AMA. If the laser beam is off-centre with respect to the centre of the curvature of the AMA, the beam may become tilted [8]. In our scheme, we measure the tilt of the laser beam with a SHWS. Figure 3a shows the influence of the vertical offset of the AMA with respect to the laser beam on its horizontal and vertical tilts. Theses measurements were conducted with a pump energy of 1.8 J on the AMA and a 300 s thermalization time.
To confirm experimental results, a propagation code with angular spectrum method has been implemented. Results of the simulation are presented in Figure 3a (lines). Figure 3b presented measurement of the evolution of the temperature of AMA (blue), radius of curvature (black), horizontal tilt (wine) and vertical tilt (green) versus time during pumping with AMA alignment optimization (cf Figure 3a).

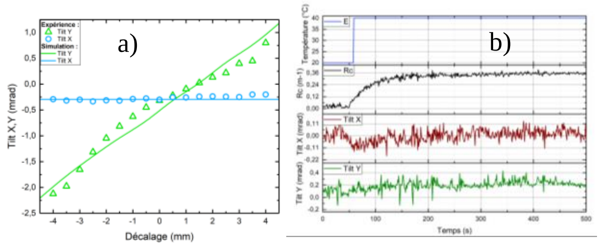

Figure 3. (a) Horizontal (green) and vertical (blue) tilt versus offset vertical offset of the AMA. Points: experimental ; Line: simulations. (b) Evolution of the temperature of AMA (blue), radius of curvature of active-mirror (black), horizontal tilt (wine) and vertical tilt (green) versus time during pumping.

These measurements show the possibility of compensating the induced vertical tilt by the rise in temperature during pumping

4 Conclusion

In this presentation, we will outline experimental performances of a 4-pass 4-active-mirrors amplifier with Nd: phosphate or Nd :Lu :CaF_2 compared to thermo-optical simulations using COMSOL [3] and propagation simulation using Miro [9].

This work was partly supported by the Conseil Régional de Nouvelle Aquitaine and the European Union through the project LEAP - Axes B et C (contracts CPER #16004205 and #DEE21-04-2019-5131820 and ERDF #2663710 and #3404410).

References

1. Pan L, Ji S, Huang W, Guo J, Lu X, Wang J, Fan W, Li X, Zhu J. *Photonics*; 8(4):96. (2021).
2. J. Guo, J. Wang, H. Wei, W. Huang, T. Huang, G. Xia, W. Fan, and Z. Lin. *High Power Laser Science and Engineering*, vol. **7**, p. e8, (2019).
3. C. Bernerd, B. Da Costa Fernandes, E. Boursier, J. Luce, C. Maunier, A. Braud, C. Meroni, P. Camy, and S. Montant. *Appl. Opt*. 59, 9905-9911 (2020).
4. D. Brown, J. Kelly, J. Abate, *IEEE Journal of Quantum Electronics*, vol. **17**, no. 9, pp. 1755-1765 (1981).
5. J. A. Abate, L. Lund, D. Brown, S. Jacobs, S. Refermat, J. Kelly, M. Gavin, J. Waldbillig, and O. Lewis. *Appl. Opt*. 20, 351-361 (1981).
6. X. Fu, Q. Liu, P. Li, Z. Sui, T. Liu, and M. Gong. *Appl. Physics*. Express, vol. **8** (2015).
7. S. Normani, A. Braud, R. Soulard, J.-L. Doualan, A. Benayad, G. Brasse, R. Moncorgé et J.-P. Goosens and P. Camy. *Cryst. Eng. Comm.,* pp. 9016-9025 (2016).
8. Z. Xiahui, and C. Xiyao. *Opt. Express,* vol **27**, pp. 1179-1198 (2019)
9. O. Morice, *Optical Enfineering*, n° %16, pp. 1530-1541 (2003).